nature immunology

# Perforin pores in the endosomal membrane trigger the release of endocytosed granzyme B into the cytosol of target cells

Jerome Thiery[1,2], Dennis Keefe[1,2], Steeve Boulant[1,3], Emmanuel Boucrot[1,3], Michael Walch[1,2], Denis Martinvalet[1,2,4], Ing Swie Goping[5], R Chris Bleackley[5], Tomas Kirchhausen[1,3] & Judy Lieberman[1,2]



**How the pore-forming protein perforin delivers apoptosis-inducing granzymes to the cytosol of target cells is uncertain. Perforin induces a transient $Ca^{2+}$ flux in the target cell, which triggers a process to repair the damaged cell membrane. As a consequence, both perforin and granzymes are endocytosed into enlarged endosomes called 'gigantosomes'. Here we show that perforin formed pores in the gigantosome membrane, allowing endosomal cargo, including granzymes, to be gradually released. After about 15 min, gigantosomes ruptured, releasing their remaining content. Thus, perforin delivers granzymes by a two-step process that involves first transient pores in the cell membrane that trigger the endocytosis of granzyme and perforin and then pore formation in endosomes to trigger cytosolic release.**

Cytotoxic T lymphocytes and natural killer (NK) cells eliminate virus-infected or malignantly transformed cells principally by releasing the contents of cytotoxic granules[1] into the immune synapse formed with their target cell[2–5]. The granule serine proteases (granzymes) induce programmed cell death[6–8] after they are delivered into the target cell cytoplasm by the pore-forming granule protein perforin[9–12]. Perforin-deficient mice are profoundly immunodeficient. They fail to eliminate many viruses and other intracellular pathogens, spontaneously develop B cell lymphoma and are highly susceptible to carcinogen-induced neoplasia[13]. Humans bearing genetic mutations that lead to impaired synthesis, function or release of perforin develop familial hemophagocytic lymphohistiocytosis[14,15].

The way that perforin delivers granzymes to the cytosol of target cells is not fully understood[16]. Perforin binds in a $Ca^{2+}$-dependent manner to membranes and multimerizes to form pores. Two models[17], both based on the membranolytic properties of perforin[18], differ in their predicted site of action. The simplest model is that granzymes are delivered directly to the cytosol by plasma membrane pores[19–22]. Cells treated with high concentrations of recombinant or purified perforin form pores that are visible by electron microscopy and are sufficiently large for granzymes to pass through. However, perforin at such high concentrations forms stable pores that kill a cell by necrosis, whereas at physiological concentrations that deliver granzymes to induce apoptosis, granzymes are taken up with perforin into endosomes rather than being delivered directly to the cytosol, as would be predicted if they entered via plasma membrane pores[23,24]. This scenario has prompted a revised model that suggests that perforin acts at the endosomal membrane by damaging its structural integrity (as originally proposed[25,26]), like some bacterial pore-forming proteins, to release granzymes to the cytosol.

At physiologically relevant, sublytic concentrations and during killer cell–mediated lysis, perforin perturbs the target plasma membrane (presumably by creating small pores in the target-cell membrane), transiently allowing $Ca^{2+}$ and small dyes to enter the target cell[23]. The $Ca^{2+}$ influx triggers the damaged membrane–repair response in which plasma membrane lesions are repaired via calcium-dependent exocytosis of lysosomes and other vesicles[27–29]. Another feature of the damaged-membrane response is the induction of endocytosis for the removal of the damaged membrane from the cell surface to preserve the integrity of the cell membrane[23,24,30]. Treatment of target cells with perforin and granzymes or killer cells leads to rapid clathrin- and dynamin-dependent endocytosis[24]. Greatly enlarged vesicles positive for early endosomal antigen 1 (EEA1)[23,24], called 'gigantosomes', are formed that contain perforin and granzymes. When the cellular membrane-repair response is inhibited by $Ca^{2+}$ chelation or inhibitors of endocytosis, treated cells die by necrosis rather than by apoptosis, which suggests that activating the membrane-repair response is critical for immune response–mediated death by apoptosis.

The aim of our study here was to investigate how gigantosomes form and how granzymes are released from them. Using live-cell imaging microscopy, we found that gigantosomes formed in target cells by GTPase Rab5–dependent homotypic fusion between EEA1-stained early endosomes. However, endosomal fusion was not essential for cell death. Moreover, perforin-induced gigantosomes did not acidify.

[1]Immune Disease Institute and Program in Cellular and Molecular Medicine, Children's Hospital, Boston, Massachusetts, USA. [2]Department of Pediatrics, Harvard Medical School, Boston, Massachusetts, USA. [3]Department of Cell Biology, Harvard Medical School, Boston, Massachusetts, USA. [4]Department of Cell Physiology and Metabolism, University of Geneva, Geneva, Switzerland. [5]Department of Biochemistry, University of Alberta, Edmonton, Alberta, Canada. Correspondence should be addressed to J.L. (lieberman@idi.harvard.edu).

Received 18 March; accepted 10 May; published online 19 June 2011; doi:10.1038/ni.2050

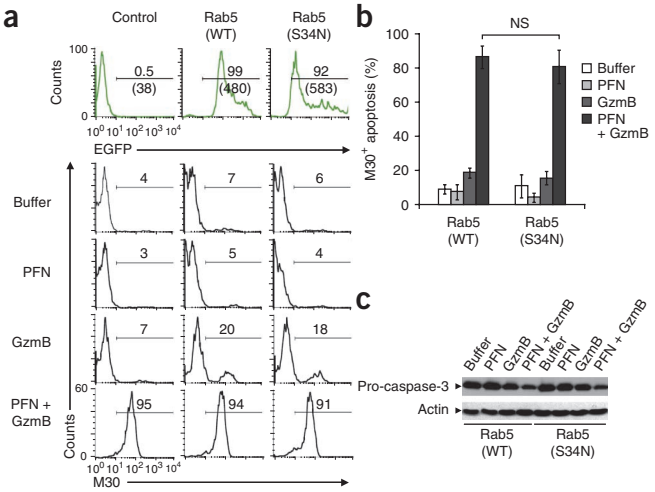


**Figure 1** Inhibition of gigantosome formation does not impair granzyme B–induced apoptosis. (**a**) Flow cytometry of eGFP in untransfected control HeLa cells or in cells transfected with plasmid encoding eGFP-tagged wild-type Rab5 (Rab5(WT)) or Rab5(S34N) (top row), then treated for 2 h with buffer or a sublytic concentration of rat perforin (PFN) or 100 nM native human granzyme B (GzmB) alone or together (PFN + GzmB) and labeled with monoclonal antibody M30 (which recognizes a cytokeratin-18 epitope after caspase cleavage) for analysis of apoptosis of eGFP$^+$ cells (below). Numbers above bracketed lines indicate percent eGFP$^+$ cells (top row) or cells that underwent apoptosis (below); numbers in parentheses below bracketed lines indicate mean fluorescence intensity. (**b**) Frequency of M30$^+$ apoptotic cells in **a**. NS, not significant (unpaired two-tailed Student's *t*-test). (**c**) Immunoblot analysis of the activation of pro-caspase-3 in HeLa cells transfected with plasmid encoding eGFP-tagged wild-type Rab5 or Rab5(S34N), then treated for 30 min with buffer or a sublytic concentration of rat perforin or 50 nM native human granzyme B alone or together. Actin serves as a loading control. Data are from three independent experiments (**a**,**b**; mean ± s.d.) or are representative of two independent experiments (**c**).

We visualized granzyme B and perforin in cells subjected to attack by NK cells. By live-cell imaging, we found that granzyme- and perforin-containing gigantosomes formed not only when cells were treated with sublytic concentrations of perforin but also during cell-mediated cytolysis. Perforin-mediated release of cargo into the cytosol occurred about 10–15 min after perforin treatment, coincident with perforin multimerization in the gigantosome membrane. Cargo release gradually occurred from discrete locations in the endosomal membrane, followed by rupture of endosomes and release of their remaining cargo.

## RESULTS

### Apoptosis without gigantosome formation

We first verified that large EEA1$^+$ intracellular vesicles (gigantosomes) that contained perforin and granzymes[23,24] formed after treatment with sublytic concentrations of perforin[23,24] (**Supplementary Fig. 1a**). These enlarged endosomes were negative for the lysosome marker CD107a (LAMP-1) and formed by homotypic fusion of early endosomes (**Supplementary Fig. 1b–e**). Rab5 is a small GTPase that regulates fusion between endocytic vesicles and early endosomes, as well as homotypic fusion between early endosomes[31–33]. Mutant Rab5 with substitution of asparagine for the serine at position 34 (Rab5(S34N)) has an affinity for GDP and acts as a dominant-negative inhibitor of Rab5 (ref. 34). In HeLa human epithelial cells transfected with plasmids encoding EEA1 tagged with monomeric red fluorescent protein and wild-type Rab5 tagged with enhanced green fluorescent protein (eGFP), gigantosomes formed within 10 min of treatment of the cells with sublytic concentrations of perforin, but they did not form when wild-type Rab5 was replaced with Rab5(S34N) (**Supplementary Fig. 2**). Thus, gigantosome formation was Rab5 dependent. We next determined whether gigantosome formation is required for the induction

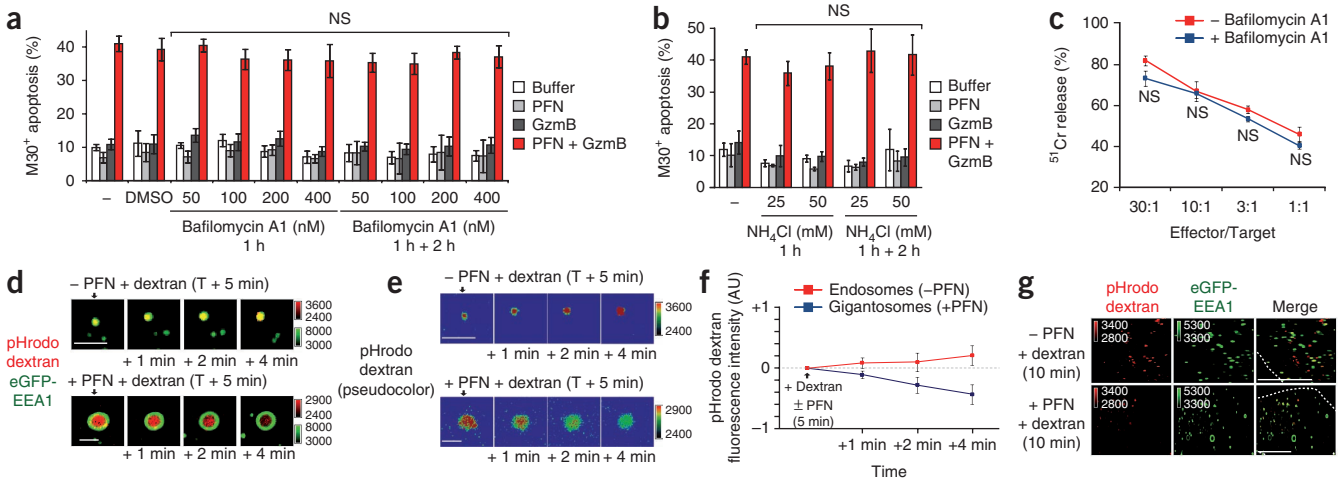


**Figure 2** Perforin inhibits endosome acidification. (**a**,**b**) Frequency of M30$^+$ apoptotic cells among HeLa cells preincubated for 1 h with bafilomycin A1 (**a**) or $NH_4Cl$ (**b**) with subsequent treatment (killing assay) for 2 h with granzyme B or a sublytic concentration of rat perforin, alone or together, with (1 h + 2 h) or without (1 h) the addition of bafilomycin A1 or $NH_4Cl$ during the killing assay. (**c**) $^{51}$Cr-release analysis of NK cell–mediated killing of 721.221 target cells with (+) or without (–) pretreatment with bafilomycin A1. (**d**) Live-cell imaging of HeLa cells expressing eGFP-tagged EEA1 (eGFP-EEA1) incubated with pHrodo dextran with or without a sublytic concentration of perforin, followed by analysis of fluorescence in normal endosomes (–PFN) or in gigantosomes (+PFN) 5 min later (T + 5 min; downward arrow); for numbers below images, time 0 is 5 min after the addition of pHrodo dextran. Color keys (right margin) indicate fluorescence intensity levels in arbitrary units throughout. Scale bars, 2 μm. (**e**) Pseudocoloring of the fluorescence intensity of pHrodo dextran in **d** (image size as in **d**). (**f**) Fluorescence intensity of pHrodo dextran in normal endosomes or gigantosomes ($n = 6$) in the cells in **d**; + Dextran ± PFN indicates dextran with or without perforin. AU, arbitrary units. (**g**) Confocal microscopy of eGFP-EEA1–transfected HeLa cells 10 min after the addition of a sublytic concentration of perforin and pHrodo dextran; dashed lines indicate plasma membrane. Scale bars, 10 μm. Data are from four (**a**,**b**) or six (**d**–**f**) independent experiments (mean ± s.d. in **a**,**b**,**f**) or are representative of two (**c**) or three (**g**) independent experiments (mean ± s.d. of triplicates in **c**).

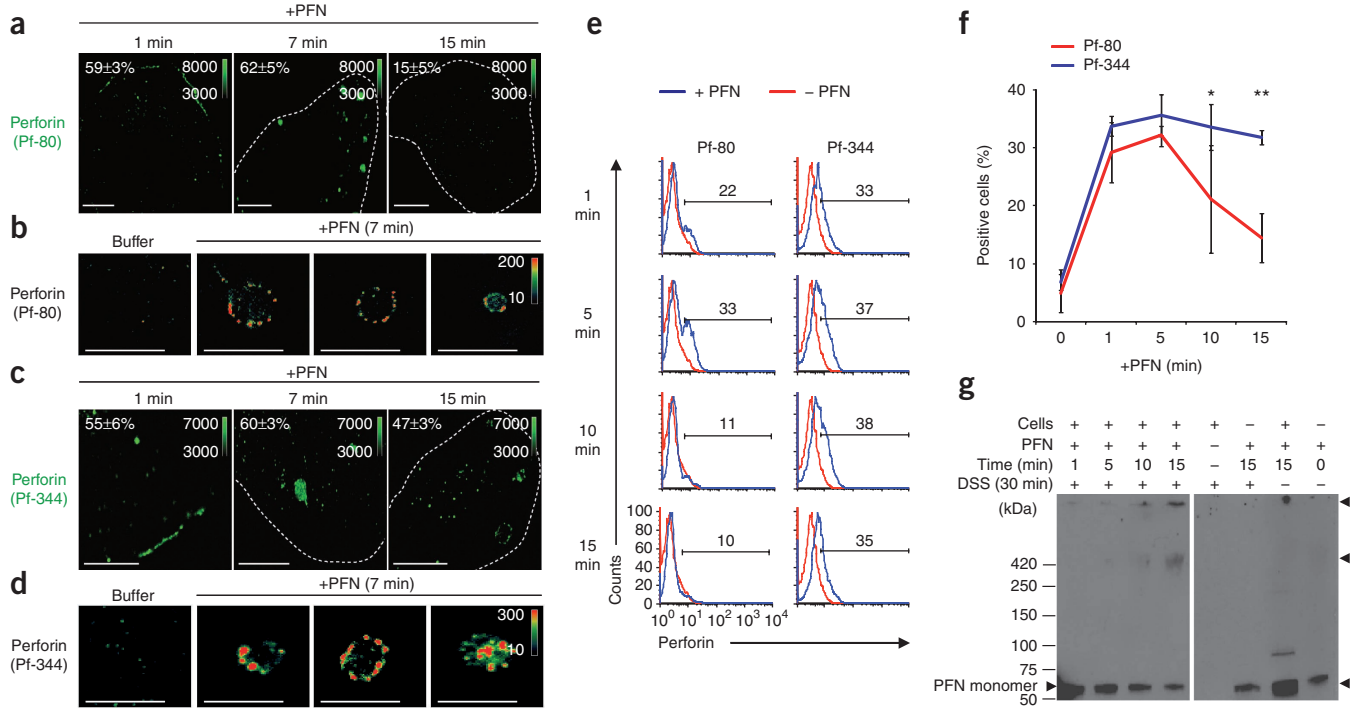


**Figure 3** Perforin multimerizes in gigantosome membranes. (**a**–**d**) Confocal microscopy of HeLa cells stained with Pf-80 (**a**,**b**) or Pf-344 (**c**,**d**) after incubation for various times (above images) with buffer or a sublytic concentration of human perforin; dashed lines indicate plasma membrane. Color bars indicate staining intensity; numbers in images (**a**,**c**) indicate percent cells with PFN staining (mean ± s.d.). Scale bars, 10 μm (**a**,**c**) or 5 μm (**b**,**d**). (**e**,**f**) Flow cytometry of HeLa cells stained with Pf-80 or Pf-344 at various times (left margin (**e**) or horizontal axis (**f**)) after incubation with a sublytic concentration of human perforin. Numbers above bracketed lines (**e**) indicate percent perforin-positive cells. $*P < 0.025$ and $**P < 0.002$ (**f**; unpaired two-tailed Student's *t*-test). (**g**) Immunoblot analysis of perforin aggregates in K562 human myelogenous leukemia cells incubated for various times (above lanes) with native human perforin, followed by the addition of the crosslinking agent disuccinimidyl suberate (DSS) for 30 min; arrowheads indicate perforin monomer (60 kDa) and perforin multimers above (~420 kDa and near top). Data are representative of at least three independent experiments (**a**–**d**,**g**), are from one experiment (**e**) or are representative of three independent experiments (**f**; mean ± s.d.).

of apoptosis by granzyme B and perforin. We assessed perforin- and granzyme B–mediated apoptosis by cleavage of cytokeratin 18 and caspase-3 and staining with annexin V and propidium iodide in HeLa cells transfected with plasmid encoding wild-type Rab5 or Rab5(S34N) (**Fig. 1** and **Supplementary Fig. 3**). Apoptosis was similar in untransfected control cells and in cells expressing wild-type Rab5 or Rab5(S34N). Thus, gigantosome formation was dispensable for granzyme B–mediated induction of apoptosis.

## Perforin inhibits early endosome acidification

Granzymes must be released into the target-cell cytosol to trigger apoptosis[23,24]. We hypothesized that granzymes are released when perforin forms endosomal membrane pores. However, early endosomes normally rapidly acidify through the actions of the vacuolar ATPase[35], and perforin pore formation is severely compromised at a pH below 6.5 (ref. 36; data not shown). We therefore predicted that perforin might interfere with endosomal acidification. We first assessed whether perforin-mediated delivery of granzyme B and induction of apoptosis required endosomal acidification by treating target cells with bafilomycin A1, an inhibitor of the vacuolar-type $H^+$-ATPase[37,38] (**Fig. 2a**) or with ammonium chloride, a weak base that increases endosomal pH by unidirectional diffusion into endosomes[39] (**Fig. 2b**). Perforin- and granzyme B–mediated apoptosis was not altered by pretreatment of HeLa cells with these agents that interfere with endosomal acidification. Similarly, preincubation of target cells with bafilomycin A1 did not affect NK cell–mediated killing (**Fig. 2c**). Moreover, pretreatment with bafilomycin A1 did not lead to more perforin-induced necrosis (**Supplementary Fig. 4a**). Therefore, delivery of granzyme B by perforin did not require endosomal acidification.

To assess whether perforin-containing gigantosomes acidify, which would interfere with pore formation by perforin in the gigantosome membrane, we treated cells with sublytic concentrations of perforin and with pHrodo dextran, which emits a bright red-fluorescent signal in an acidic environment. In cells treated with pHrodo dextran without perforin, endosomal red fluorescence increased over a few minutes, as expected. However, in cells treated with sublytic concentrations of perforin, red fluorescence in the gigantosomes progressively decreased with time (**Fig. 2d**–**f**). Within 10 min, most gigantosomes did not show any red fluorescence, unlike normal endosomes in the same cell or in cells not exposed to perforin (**Fig. 2g**). Thus gigantosomes did not acidify like normal endosomes. The lack of gigantosome acidification may have been due to perforin pore formation in the gigantosome membrane, which would interfere with the maintenance of a pH gradient across the gigantosome membrane. To confirm the data above, we also co-treated cells with perforin and the ratiometric probe Lysosensor Yellow/Blue, which fluoresces in the green channel only at low pH. At the earliest times, Lysosensor Yellow/Blue fluorescence was similar in perforin-treated and control cells, which suggested that their dye uptake was equivalent (data not shown). However, cells treated with sublytic concentrations of perforin demonstrated a rapid progressive decrease in Lysosensor Yellow/Blue green fluorescence over 5 min, whereas the fluorescence in cells treated with medium did not change. Moreover, the lower fluorescence was not due to leakage of dye from the cell, as plasma membrane integrity,

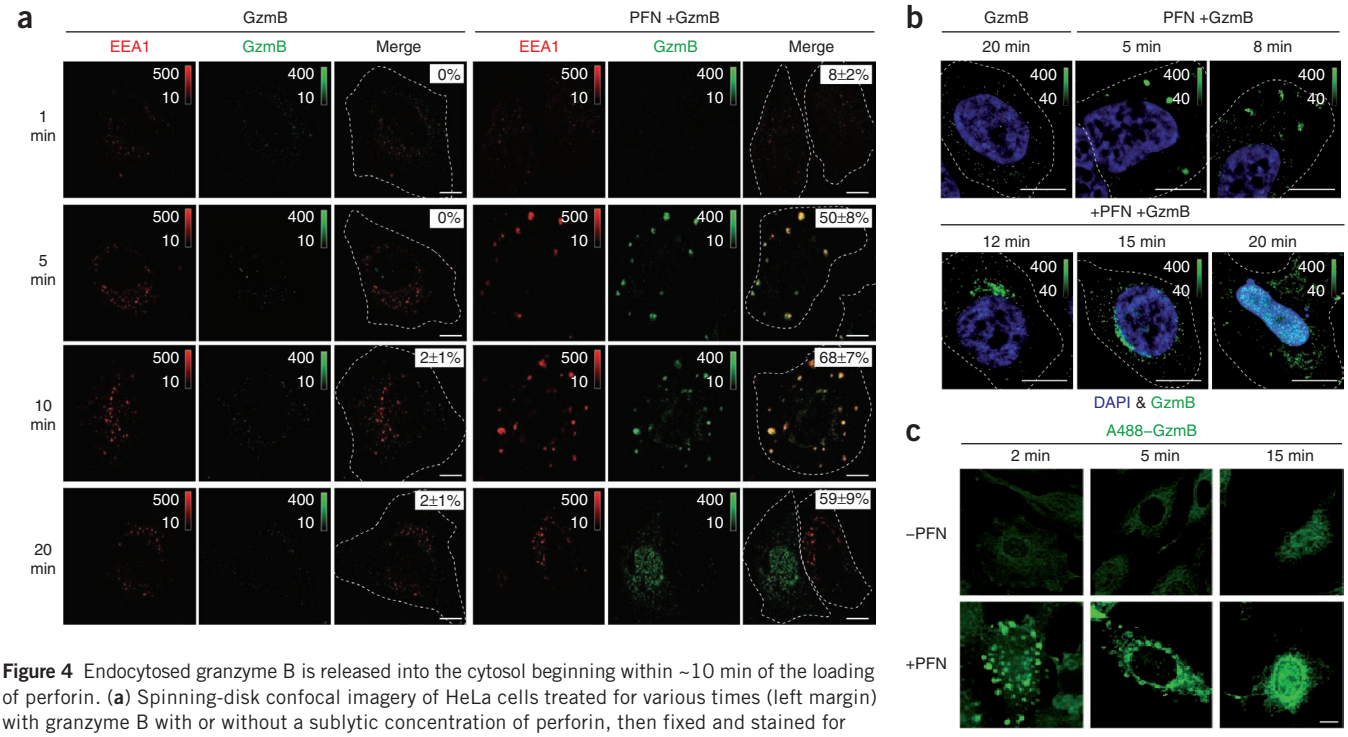


**Figure 4** Endocytosed granzyme B is released into the cytosol beginning within ~10 min of the loading of perforin. (**a**) Spinning-disk confocal imagery of HeLa cells treated for various times (left margin) with granzyme B with or without a sublytic concentration of perforin, then fixed and stained for EEA1 and granzyme B. Numbers in images (top right corner; Merge) indicate percent cells with granzyme B in gigantosomes or in the cytosol (mean ± s.d.). (**b**) Microscopy of HeLa cells treated for various times (above images) with native human granzyme B with or without a sublytic concentration of rat perforin, then fixed and stained for granzyme B and with the DNA-intercalating dye DAPI; images were acquired by three-dimensional capture widefield microscopy followed by iterative deconvolution and projection. (**c**) Microscopy of HeLa cells treated for various times (above images) with Alexa Fluor–labeled granzyme B (A488-GzmB) with or without a sublytic concentration of perforin (left margin), then fixed. Dashed lines (**a**,**b**) indicate plasma membrane; color bars indicate fluorescence intensity. Scale bars, 5 μm (**a**) or 10 μm (**b**,**c**). Data are from three independent experiments (**a**) or are representative of three (**b**) or two (**c**) independent experiments.

assessed by lack of uptake of propidium iodide, remained unimpaired (**Supplementary Fig. 4b**). Thus, gigantosomes that formed in perforin-treated cells did not acidify.

### Perforin forms pores in the endosomal membrane

The most likely explanation for perforin permeabilization of the gigantosome membrane was that perforin forms pores in the gigantosome membrane. We treated target cells with perforin and stained them 7 min later with the Pf-80 monoclonal antibody to human perforin, used before for visualization of perforin in target cell gigantosomes[24]; this confirmed the localization of perforin in gigantosomes (**Fig. 3a**). High-magnification images of gigantosomes stained with Pf-80 7 min after the addition of perforin showed highly localized perforin staining in clumps on the endosomal membrane (**Fig. 3b** and **Supplementary Fig. 5a**,**b**), as might be expected to form as perforin multimerizes to form pores. However, Pf-80 staining became almost completely undetectable 15 min after perforin was loaded. Pf-80 recognizes an epitope that is exposed in monomeric perforin and in the first step of the binding of perforin to membranes, but staining disappears when perforin multimerizes to form transmembrane pores[40]. The disappearance of perforin staining could be due either to the formation of perforin pores or to degradation of perforin in the target cell. However, staining of perforin with monoclonal antibody Pf-344, which recognizes an epitope that remains exposed throughout the various steps in perforin pore formation[40], was still detectable even 15 min later (**Fig. 3c**,**d** and **Supplementary Fig. 5c**). Similarly, by flow cytometry, staining of perforin-treated cells with Pf-80 was visible 5 min after the addition of perforin but was no longer detectable at 10 or 15 min, whereas staining with Pf-344 persisted for as long as it was measured (15 min; **Fig. 3e**,**f**). Therefore perforin was not degraded; instead, staining of perforin with Pf-80 disappeared because perforin formed pores in the gigantosome membrane. To confirm that finding, we next assessed whether we could detect perforin multimers in target cells with chemical crosslinking (**Fig. 3g**). We incubated target cells for 1–15 min with a sublytic concentration of native human perforin before adding the membrane-permeable crosslinking agent disuccinimidyl suberate. Immunoblot analysis of perforin in the lysates of crosslinked cells showed a gradual decrease of the 60-kilodalton (60-kDa) perforin monomer, whereas two crosslinked bands appeared after 10 min and increased in intensity at 15 min. The lower band had an estimated size of ~420 kDa, consistent with the size of a perforin heptamer, and the top band migrated near the top of the gel, which suggested the formation of a much larger multimer. At these time points, perforin staining was almost exclusively present in endosomes[24] (**Fig. 3a**,**c**), which suggested that pore formation occurs in endosomal membranes. When we fractionated perforin-treated cells to isolate cytoplasmic vesicles before crosslinking with disuccinimidyl suberate, we also found crosslinked bands of the same size (**Supplementary Fig. 5d**). Thus, perforin pore formation increases over time in the gigantosome membrane.

### Release of granzyme B and other cargo from gigantosomes

To test our hypothesis that perforin pore formation in the endosomal membrane is responsible for granzyme release, we co-stained for EEA1 and granzyme B and assessed the timing of granzyme B uptake and cytosolic release after treatment with perforin and granzyme B. In the absence of perforin, cells did not efficiently

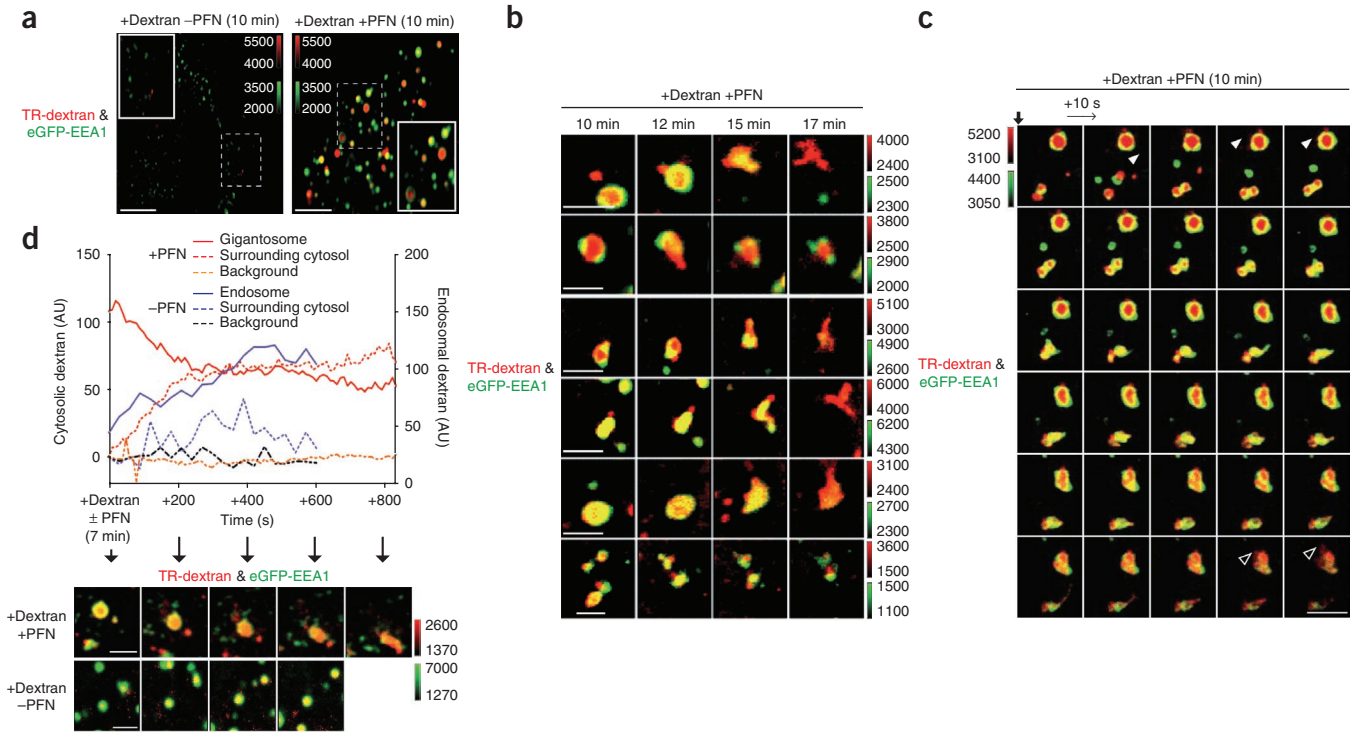


**Figure 5** Release of endocytosed cargo from gigantosomes into the cytosol. (**a**) Microscopy of the uptake of TR-dextran in HeLa cells transfected with plasmid encoding eGFP-EEA1 and left untreated (–PFN) or treated for 10 min with a sublytic concentration of perforin (+PFN). (**b**) Microscopy of the release of dextran from gigantosomes in HeLa cells transfected with plasmid encoding eGFP-EEA1 and incubated for 10–17 min with TR-dextran and a sublytic concentration of perforin. (**c**) Time-lapse confocal microscopy of eGFP-EEA1$^+$ HeLa cells, acquired every 10 s beginning 10 min after treatment with TR-dextran and a sublytic concentration of perforin (source, **Supplementary Movie 1**). White arrowheads indicate discrete release of TR-dextran; open arrowheads indicate dextran dispersal after gigantosome rupture. (**d**) Intensity of dextran in a perforin-induced gigantosome (+PFN) or in a normal endosome (–PFN; right vertical axis) and in the local surrounding area (left vertical axis) of HeLa cells beginning 7 min after treatment with TR-dextran with or without a sublytic concentration of perforin (+Dextran ± PFN); background intensity was measured in a region devoid of gigantosomes and endosomes. Below, images corresponding to the data above. Color bars indicate fluorescence intensity. Scale bars, 5 μm (**a**) or 2 μm (**b**–**d**). Data are representative of six (**a**), five (**b**) or three (**c**) independent experiments.

take up granzyme B (**Fig. 4a**). After exposure to sublytic concentrations of perforin and granzyme B, granzyme B–containing EEA1$^+$ gigantosomes formed within 5 min. After ~10–15 min, granzyme B was released from gigantosomes to the cytosol, as the bright vesicular staining of the endocytosed cargo dispersed into a faintly detected haze in the cytosol. Within 20 min, most of the granzyme B signal was concentrated in the nucleus, as expected[41], and we no longer detected gigantosomes (**Fig. 4a**,**b**). We also noted uptake of Alexa Fluor 488–granzyme B into gigantosomes within 2 min of adding perforin. Cytosolic fluorescence began to be visible within 5 min, but by 15 min, gigantosome staining had disappeared and granzyme B became cytosolic and nuclear (**Fig. 4c**). Therefore, the release of granzyme B from gigantosomes in perforin-treated cells within ~15 min coincided temporally with perforin pore formation, as judged by the disappearance of Pf-80 staining and perforin crosslinking.

## Gigantosomes leak cargo and then rupture

We next used live-cell imaging to visualize the release of gigantosome cargo from perforin-treated cells. We used time-lapse spinning-disk confocal microscopy to image trafficking of the 10-kDa fluid-phase endocytosis marker Texas red–dextran (TR-dextran) in perforin-treated HeLa cells transfected to express eGFP-tagged EEA1. As described before[24], perforin enhanced the endocytosis of TR-dextran, and TR-dextran remained located in gigantosomes after 10 min (**Fig. 5a**). We obtained similar results with cells transfected with monomeric red fluorescent protein–tagged EEA-1 and treated with dextran tagged with 10-kDa cationic rhodamine green and perforin (data not shown). After 10 min, we began to observe discrete and localized release of TR-dextran from gigantosomes into the cytosol, whereas the gigantosome membrane seemed to remain intact (**Fig. 5b** and **Supplementary Fig. 6a**). A little later (~15–17 min after loading of perforin–TR-dextran), the gigantosome membrane became unstable. EEA1 coating of gigantosomes disappeared and endosomal tubulations formed, which was followed by rupture of the gigantosome membrane, leading to complete release and diffusion of dextran into the cytosol (**Fig. 5b**,**c**, **Supplementary Fig. 6b** and **Supplementary Movies 1**–**3**). As dextran diffuses, it becomes difficult to detect. To confirm our impression that TR-dextran was released from gigantosomes into the cytosol before they ruptured, we imaged perforin- and dextran-treated cells by live-cell four-dimensional spinning-disk confocal imaging beginning 7 min after the addition of perforin and dextran. We measured the staining intensity of TR-dextran in the gigantosome or endosomes and in their surrounding cytoplasm (**Fig. 5d**). In the absence of perforin, the TR-dextran signal in endosomes gradually increased as more dextran was incorporated, but the signal in the surrounding cytosol remained low and was stable, with some fluctuation. However, in cells treated with perforin, the signal intensity of TR-dextran in the gigantosome gradually decreased as Texas red staining in the surrounding cytoplasm increased. As a

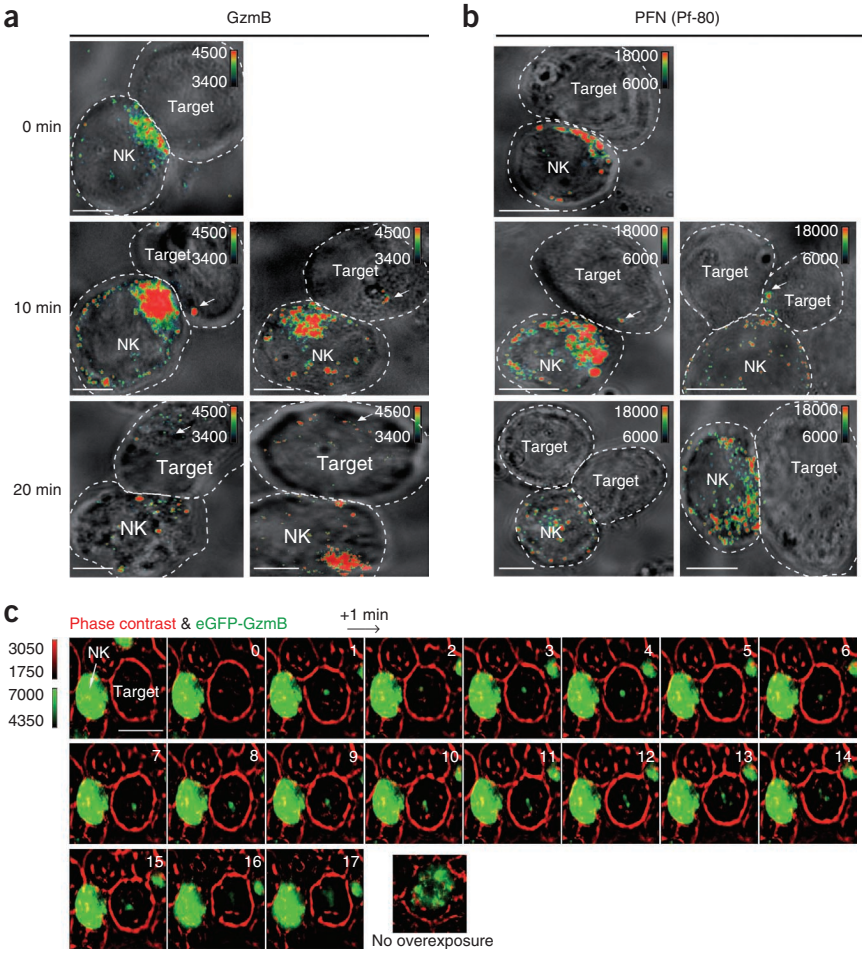


**Figure 6** Granzyme B and perforin localize in gigantosomes in target cells during lysis by NK cells. (**a**,**b**) Spinning-disk confocal microscopy (*z*-stack series projections) of YT-Indy NK cells incubated for various times (left margin) with 721.221 target cells, then stained for granzyme B (**a**) or perforin (**b**). Arrows indicate granzyme B or perforin signal (pseudocolor) in target cells; dashed lines indicate plasma membrane. (**c**) Widefield live imaging (time-lapse series) of YT-Indy NK cells expressing eGFP–granzyme B (eGFP-GzmB) incubated with 721.221 target cells and imaged every minute (numbers in top right corners indicate time (in min) after conjugate formation). Phase contrast is red. For visualization of the low granzyme B signal in the target cell, the eGFP channel was overexposed. Bottom row right (No overexposure), control YT-Indy cell imaged with normal exposure time to confirm the granular expression of eGFP–granzyme B. Color bars indicate fluorescence intensity. Scale bars, 10 μm. Data are representative of two independent experiments.

control, we measured the background intensity of TR-dextran staining in a region of the cytosol that did not contain gigantosomes or endosomes and found that it did not change. Together these data suggest that perforin pores in the gigantosome membrane allow the slow release of endosomal cargo before completely destabilizing the endosomal membrane, which leads to endosomolysis and rapid release of the remaining cargo to the cytosol (model for perforin delivery of granzymes, **Supplementary Fig. 7**).

### Release of granzyme B from gigantosomes during NK cell attack

The most physiologically relevant system with which to study the actions of perforin is lysis of target cells mediated by cytotoxic T lymphocytes or NK cells. However, no published studies have visualized trafficking of perforin or granzyme in cells subjected to killer cell–mediated destruction, presumably because the amount of native enzyme that enters a target cell is limited. We obtained the data presented above by incubating target cells with sublytic concentrations of perforin (with or without granzyme B), which is considered a good surrogate for killer cell–mediated cell death, as it reproduces the apoptotic features of the target cell. The two components of the cellular membrane-repair response (fusion of internal vesicles with the plasma membrane and rapid endocytosis of the damaged membrane) are present in cells targeted by $CD8^+$ T cells and NK cells[23,24]. Moreover, $EEA1^+$ gigantosomes form in target cells during killer cell attack[23,24]. To assess further whether the two-step model of the delivery of granzyme by perforin via endosomes applies to the physiologically most relevant model of killer cell attack, we incubated the human NK cell line YT-Indy with 721.221 human B cells (as target cells) and examined NK cell–target cell conjugates at various times over 20 min on slides stained for granzyme B or perforin. In NK cells, granzyme B and perforin stained in granules that concentrated at the interface with the target cell, as expected (**Fig. 6a**,**b**). Although staining of granzyme B or perforin was not apparent in most target cells, at 10 min, we were able to visualize in a few cells granzyme B and perforin in enlarged cytosolic vesicles with a size like that of gigantosomes. Target cells with staining of granzyme B or perforin typically had one or a few gigantosomes visible near the killer cell–target cell interface. After 20 min of incubation, we detected dispersion of granzyme B in the cytosol of a few target cells. At the same time, we did not detect perforin staining with the conformation-sensitive antibody Pf-80 in any target cell (**Fig. 6b**). To monitor granzyme B trafficking in target cells, we also imaged YT-Indy cells that expressed eGFP–granzyme B as they targeted 721.221 cells (**Fig. 6c**). We found that eGFP–granzyme B first concentrated in a gigantosome-like structure that was visible within a minute of conjugate formation before dispersing in the cytosol ~10–17 min later. Therefore, endocytosis of granzyme B and perforin into gigantosomes and perforin-induced release of granzyme B from gigantosomes into the cytosol of target cells also occurred during attack by killer cells.

## DISCUSSION

At physiologically relevant concentrations of perforin and during attack by cytotoxic T lymphocytes, perforin creates short-lived pores in the plasma membrane of the target cell. These pores cause a transient influx of $Ca^{2+}$ into the target cell that lasts a few hundred seconds and mobilizes the stereotypic cellular response to plasma membrane damage[23]. The membrane-repair response, which is triggered by an increase in intracellular $Ca^{2+}$ concentration, mends the damaged plasma membrane by the fusion of lysosomal and endosomal membranes[23,30] and by endocytosis to remove the damaged membrane[24]. The stimulation of endocytosis leads to the internalization of perforin and granzymes into early endosomes[24]. In cells treated with physiologically relevant, sublytic concentrations of perforin, we observed

the formation of giant endosomes (gigantosomes) that contained perforin and granzymes. We also noted enlarged EEA1$^+$ vesicles in target cells during attack by killer cells. A hallmark of the membrane-repair response is exuberant heterotypic and homotypic fusion caused by $Ca^{2+}$-dependent activation of vesicular trafficking molecules, such as the synaptotagmins and SNARE proteins[27–29]. We found that gigantosomes formed by Rab5-dependent fusion of early endosomes. However, gigantosome formation was an extraneous phenomenon that did not contribute to killing of target cells. As target cells that did not form gigantosomes were equally susceptible to granzyme B and perforin, these results suggest that granzymes also escape from smaller granzyme- and perforin-containing endosomes via the action of perforin in endosomes. Although we saw granzymes in endosomes within a few minutes of exposure to perforin, granzymes were present in the cytosol only much later (~15 min after treatment). This result suggested that the pores formed by perforin in the plasma membrane were either too small or too rapidly removed to deliver granzymes directly to the cytosol.

We next investigated how gigantosome cargo is delivered to the cytosol. We found that granzymes and other cargo were released into the cytosol through the action of perforin in the gigantosome membrane. Imaging of cells treated with perforin and granzymes showed perforin concentrated in discrete foci that formed on the gigantosome membrane, which suggested that perforin forms pores in the endosomal membrane. However, perforin pore formation does not occur at an acidic pH[36]. Here we found that unlike normal early endosomes[35], gigantosomes did not acidify, thereby facilitating perforin pore formation in the gigantosome. The lack of acidification was probably secondary to perforin pore formation, which would interfere with the maintenance of a pH gradient across the gigantosome membrane and would lead to equilibration of the gigantosome pH with the neutral cytosolic pH. In further support of the proposal of perforin pore formation in the gigantosome membrane, staining of gigantosomes with the perforin antibody Pf-80, which recognizes an epitope obscured during pore formation[40], disappeared. This lack of staining was not due to degradation of perforin, as staining with Pf-344, an antibody that recognizes both monomeric and multimerized perforin, persisted. Moreover, crosslinking studies showed that perforin assembled into larger complexes in gigantosomes over 15 min, coincident with the release of gigantosome cargo. Crosslinking analysis suggested that there might be two types of perforin pores: a smaller multimer made up of about seven perforin monomers, and a much larger multimer of indeterminate size. However, that finding needs to be confirmed by other methods. We imaged fluorescent cargo (fluorescence-labeled and unlabeled granzyme B and fluorescence-labeled dextran) as it was released from gigantosomes. Cargo was first released at a slow but steady rate beginning ~10 min after cells were exposed to perforin. After ~15 min, the endosomal membrane developed tubulations and eventually ruptured, which led to the complete release of cargo. Notably, treatment of cells with the vacuolar ATPase inhibitor bafilomycin A, which like perforin prevents endosomal acidification, also causes endosomal tubulations like those we visualized with perforin[42]. It is not clear what triggers the final rupture of the gigantosome or what proportion of granzyme B might be released via pores versus at the time of gigantosome lysis. The release of 10-kDa dextran, which we measured before rupture, may not exactly mimic what happens with 32-kDa granzyme B or the granzyme A dimer, which is twice as large. Given the results of live-cell imaging of perforin-treated cells, it is likely that most granzyme release occurs at the time of gigantosome rupture. Our images of granzyme B in NK cell–targeted cells also suggested that some granzyme B was released before gigantosome rupture, but the resolution of the images was not good enough to be certain.

In our studies of perforin loading of granzymes and killer cell lysis by staining of fixed cells or by videomicroscopy, we never saw evidence of the entry of granzyme directly into the cytosol via the plasma membrane. We therefore think this is unlikely. However, we cannot rule out the possibility that small amounts of granzymes entered through transient plasma membrane pores but were not detected because they diffused rapidly and the fluorescent signal was not concentrated enough to be detected above background. The response of damaged plasma membranes to bacterial pore-forming toxins and complement has been shown to include blebbing or exocytosis of damaged membranes[43,44] in addition to the two phenomena we found in cells exposed to sublytic concentrations of perforin (patching by fusion of vesicular membranes and endocytosis of damaged membrane[23,24]). In some cells, blebbing of the plasma membrane is a prominent feature after treatment with sublytic concentrations of perforin and granzymes. Examination of culture supernatants of targeted cells for granzyme- and perforin-containing exosomes may indicate whether exocytosis of perforin-damaged membranes is prominent in some cells and promotes apoptotic cell death.

Our results suggest a two-step model for the delivery of granzymes by perforin in which perforin first forms transient pores in the target-cell plasma membrane that trigger the membrane-repair response, leading to the endocytosis of granzymes and perforin together. Perforin then forms larger, more stable pores in the endosomal membrane to trigger the release of granzymes. Although we used granzyme B in the experiments presented here, we obtained similar results when we studied granzyme A, the other main granzyme (data not shown). Therefore, we expect that this model applies to all granzymes. This model, which suggests that perforin can form at least two types of pores of different size and stability, is supported by a published study that measured conductance through various sorts of membranes (planar lipid bilayers and unilamellar vesicles of different lipid composition and size) treated with perforin[45]. There was a good deal of heterogeneity in perforin pores; in particular, the formation of small, highly unstable pores preceded the development of more stable and larger pores with a distribution in size. Heterogeneous pore formation was confirmed by cryoelectron microscopy. We therefore hypothesize that the rapid membrane-repair response interferes with the formation of larger pores on the plasma membrane but that perforin multimerizes into larger stable pores on the gigantosome membrane that increase in size within 5–15 min of the addition of perforin. Given the kinetics of early endosome acidification, our data suggest that the smaller pores formed in the gigantosome membrane almost immediately to interfere with acidification and allow perforin to remain active.

Our evidence for replacing the old model of granzyme delivery through plasma membrane pores with a more complicated two-step model of perforin delivery is based mostly on experiments using treatment of target cells with perforin and granzyme at sublytic concentrations of perforin, which is considered a good model for cell-mediated cytotoxicity. It could be argued, however, that what happens during attack by killer cells might be different. During perforin- and granzyme-loading experiments, the killer molecules are delivered across the plasma membrane, whereas in cell-mediated lysis, perforin and granzymes are delivered to a localized area of the target cell membrane in the immunosynapse. The repair of diffuse membrane damage might become more important in the former case than in the latter, when membrane damage is localized. Until now it has been impossible to visualize perforin and granzymes in target cells undergoing

attack by killer cells, which has made it difficult to assess whether it is really necessary to revise the old plasma membrane pore model. $EEA1^+$ gigantosomes do in fact form in the target cell during attack by cytotoxic T lymphocytes[23,24]. Because of the improved imaging resolution of the highly sensitive spinning-disk confocal microscope, we were able to detect granzyme B and perforin in target cells as they were being killed. The killer molecules did in fact localize rapidly to giant endosomes that formed near the immune synapse before they were detected throughout the cytosol. Rather than the formation of multiple gigantosomes, as was seen in cells treated with perforin and granzyme B in solution, presumably in response to diffuse membrane damage, it is likely that only one gigantosome or a few gigantosomes form when the damage is localized to the immune synapse. The concentration of perforin and granzyme in gigantosomes in target cells followed by granzyme release during attack by killer cells suggests that the two-step model for the delivery of granzymes by perforin accurately reflects what happens *in vivo*.

## METHODS

Methods and any associated references are available in the online version of the paper at http://www.nature.com/natureimmunology/.

*Note: Supplementary information is available on the Nature Immunology website.*

### ACKNOWLEDGMENTS

We thank Y. Jones (University of Oxford) for the mammalian expression vector pHLseq; G.M. Griffiths (Oxford University) for 2d4 mouse antibody to human perforin; and E. Marino for assistance with microscopy and image analysis. Supported by the US National Institutes of Health (AI063430 to J.L. and GM075252 to T.K.), the Canadian Institutes of Health Research (R.C.B.), the Canadian Cancer Society (RCB), the Stiefel-Zangger Foundation (M.W.), the Human Frontier Science Program Organization (E.B.), the Harvard Digestive Diseases Center (S.B.) and the Immune Disease Institute and GlaxoSmithKline Alliance (S.B.).

### AUTHOR CONTRIBUTIONS

J.T. designed and did experiments, analyzed data and wrote the manuscript; S.B., D.K. and E.B. did and helped analyze some experiments; M.W. and D.M. purified granzyme B and helped with perforin purification; I.S.G. and R.C.B. developed the NK cell line expressing eGFP–granzyme B; and T.K. and J.L. conceived of and supervised the project, helped design experiments and coordinated the writing of the manuscript.

### COMPETING FINANCIAL INTERESTS

The authors declare no competing financial interests.

Published online at http://www.nature.com/natureimmunology/.
Reprints and permissions information is available online at http://www.nature.com/reprints/index.html.



1. de Saint Basile, G., Menasche, G. & Fischer, A. Molecular mechanisms of biogenesis and exocytosis of cytotoxic granules. *Nat. Rev. Immunol.* **10**, 568–579 (2010).
2. Grakoui, A. *et al.* The immunological synapse: a molecular machine controlling T cell activation. *Science* **285**, 221–227 (1999).
3. Stinchcombe, J.C., Bossi, G., Booth, S. & Griffiths, G.M. The immunological synapse of CTL contains a secretory domain and membrane bridges. *Immunity* **15**, 751–761 (2001).
4. Lieberman, J. The ABCs of granule-mediated cytotoxicity: new weapons in the arsenal. *Nat. Rev. Immunol.* **3**, 361–370 (2003).
5. Dustin, M.L. & Long, E.O. Cytotoxic immunological synapses. *Immunol. Rev.* **235**, 24–34 (2010).
6. Anthony, D.A., Andrews, D.M., Watt, S.V., Trapani, J.A. & Smyth, M.J. Functional dissection of the granzyme family: cell death and inflammation. *Immunol. Rev.* **235**, 73–92 (2010).
7. Bovenschen, N. & Kummer, J.A. Orphan granzymes find a home. *Immunol. Rev.* **235**, 117–127 (2010).
8. Lieberman, J. Granzyme A activates another way to die. *Immunol. Rev.* **235**, 93–104 (2010).
9. Pasternack, M.S. & Eisen, H.N. A novel serine esterase expressed by cytotoxic T lymphocytes. *Nature* **314**, 743–745 (1985).
10. Podack, E.R., Young, J.D. & Cohn, Z.A. Isolation and biochemical and functional characterization of perforin 1 from cytolytic T-cell granules. *Proc. Natl. Acad. Sci. USA* **82**, 8629–8633 (1985).
11. Gershenfeld, H.K. & Weissman, I.L. Cloning of a cDNA for a T cell-specific serine protease from a cytotoxic T lymphocyte. *Science* **232**, 854–858 (1986).
12. Bleackley, R.C. *et al.* The isolation and characterization of a family of serine protease genes expressed in activated cytotoxic T lymphocytes. *Immunol. Rev.* **103**, 5–19 (1988).
13. van den Broek, M.E. *et al.* Decreased tumor surveillance in perforin-deficient mice. *J. Exp. Med.* **184**, 1781–1790 (1996).
14. Stepp, S.E. *et al.* Perforin gene defects in familial hemophagocytic lymphohistiocytosis. *Science* **286**, 1957–1959 (1999).
15. Katano, H. & Cohen, J.I. Perforin and lymphohistiocytic proliferative disorders. *Br. J. Haematol.* **128**, 739–750 (2005).
16. Pipkin, M.E. & Lieberman, J. Delivering the kiss of death: progress on understanding how perforin works. *Curr. Opin. Immunol.* **19**, 301–308 (2007).
17. Voskoboinik, I., Smyth, M.J. & Trapani, J.A. Perforin-mediated target-cell death and immune homeostasis. *Nat. Rev. Immunol.* **6**, 940–952 (2006).
18. Baran, K. *et al.* The molecular basis for perforin oligomerization and transmembrane pore assembly. *Immunity* **30**, 684–695 (2009).
19. Podack, E.R. & Dennert, G. Assembly of two types of tubules with putative cytolytic function by cloned natural killer cells. *Nature* **302**, 442–445 (1983).
20. Podack, E.R., Konigsberg, P.J., Acha-Orbea, H., Pircher, H. & Hengartner, H. Cytolytic T-cell granules: biochemical properties and functional specificity. *Adv. Exp. Med. Biol.* **184**, 99–119 (1985).
21. Trapani, J.A. *et al.* Genomic organization of the mouse pore-forming protein (perforin) gene and localization to chromosome 10. Similarities to and differences from C9. *J. Exp. Med.* **171**, 545–557 (1990).
22. Tschopp, J., Masson, D. & Stanley, K.K. Structural/functional similarity between proteins involved in complement- and cytotoxic T-lymphocyte-mediated cytolysis. *Nature* **322**, 831–834 (1986).
23. Keefe, D. *et al.* Perforin triggers a plasma membrane-repair response that facilitates CTL induction of apoptosis. *Immunity* **23**, 249–262 (2005).
24. Thiery, J. *et al.* Perforin activates clathrin- and dynamin-dependent endocytosis, which is required for plasma membrane repair and delivery of granzyme B for granzyme-mediated apoptosis. *Blood* **115**, 1582–1593 (2010).
25. Froelich, C.J. *et al.* New paradigm for lymphocyte granule-mediated cytotoxicity. Target cells bind and internalize granzyme B, but an endosomolytic agent is necessary for cytosolic delivery and subsequent apoptosis. *J. Biol. Chem.* **271**, 29073–29079 (1996).
26. Browne, K.A. *et al.* Cytosolic delivery of granzyme B by bacterial toxins: evidence that endosomal disruption, in addition to transmembrane pore formation, is an important function of perforin. *Mol. Cell. Biol.* **19**, 8604–8615 (1999).
27. Reddy, A., Caler, E.V. & Andrews, N.W. Plasma membrane repair is mediated by $Ca^{2+}$-regulated exocytosis of lysosomes. *Cell* **106**, 157–169 (2001).
28. McNeil, P.L. & Steinhardt, R.A. Plasma membrane disruption: repair, prevention, adaptation. *Annu. Rev. Cell Dev. Biol.* **19**, 697–731 (2003).
29. McNeil, P.L. & Kirchhausen, T. An emergency response team for membrane repair. *Nat. Rev. Mol. Cell Biol.* **6**, 499–505 (2005).
30. Idone, V. *et al.* Repair of injured plasma membrane by rapid $Ca^{2+}$-dependent endocytosis. *J. Cell Biol.* **180**, 905–914 (2008).
31. Bucci, C. *et al.* The small GTPase rab5 functions as a regulatory factor in the early endocytic pathway. *Cell* **70**, 715–728 (1992).
32. Olkkonen, V.M. & Stenmark, H. Role of Rab GTPases in membrane traffic. *Int. Rev. Cytol.* **176**, 1–85 (1997).
33. Armstrong, J. How do Rab proteins function in membrane traffic? *Int. J. Biochem. Cell Biol.* **32**, 303–307 (2000).
34. Li, G., Barbieri, M.A., Colombo, M.I. & Stahl, P.D. Structural features of the GTP-binding defective Rab5 mutants required for their inhibitory activity on endocytosis. *J. Biol. Chem.* **269**, 14631–14635 (1994).
35. Forgac, M. Vacuolar ATPases: rotary proton pumps in physiology and pathophysiology. *Nat. Rev. Mol. Cell Biol.* **8**, 917–929 (2007).
36. Tschopp, J. & Masson, D. Inhibition of the lytic activity of perforin (cytolysin) and of late complement components by proteoglycans. *Mol. Immunol.* **24**, 907–913 (1987).
37. Yoshimori, T., Yamamoto, A., Moriyama, Y., Futai, M. & Tashiro, Y. Bafilomycin A1, a specific inhibitor of vacuolar-type $H^+$-ATPase, inhibits acidification and protein degradation in lysosomes of cultured cells. *J. Biol. Chem.* **266**, 17707–17712 (1991).
38. Recchi, C. & Chavrier, P. V-ATPase: a potential pH sensor. *Nat. Cell Biol.* **8**, 107–109 (2006).
39. Galloway, C.J., Dean, G.E., Marsh, M., Rudnick, G. & Mellman, I. Acidification of macrophage and fibroblast endocytic vesicles in vitro. *Proc. Natl. Acad. Sci. USA* **80**, 3334–3338 (1983).
40. Praper, T. *et al.* Human perforin permeabilizing activity, but not binding to lipid membranes, is affected by pH. *Mol. Immunol.* **47**, 2492–2504 (2010).
41. Jans, D.A., Jans, P., Briggs, L.J., Sutton, V. & Trapani, J.A. Nuclear transport of granzyme B (fragmentin-2). Dependence of perforin in vivo and cytosolic factors in vitro. *J. Biol. Chem.* **271**, 30781–30789 (1996).
42. D'Arrigo, A., Bucci, C., Toh, B.H. & Stenmark, H. Microtubules are involved in bafilomycin A1-induced tubulation and Rab5-dependent vacuolation of early endosomes. *Eur. J. Cell Biol.* **72**, 95–103 (1997).
43. Husmann, M. *et al.* Elimination of a bacterial pore-forming toxin by sequential endocytosis and exocytosis. *FEBS Lett.* **583**, 337–344 (2009).
44. Pilzer, D., Gasser, O., Moskovich, O., Schifferli, J.A. & Fishelson, Z. Emission of membrane vesicles: roles in complement resistance, immunity and cancer. *Springer Semin. Immunopathol.* **27**, 375–387 (2005).
45. Praper, T. *et al.* Human perforin employs different avenues to damage membranes. *J. Biol. Chem.* **286**, 2946–2955 (2010).

## ONLINE METHODS

**Purification of perforin and granzyme B.** Native human perforin and granzyme B were purified from YT-Indy NK cells and native rat perforin was purified from the RNK-16 rat natural killer cell line as described[46]. Animal use was approved by the Animal Care and Use Committees of the Immune Disease Institute and Harvard Medical School. Recombinant granzyme B was produced with the mammalian expression vector pHLseq[47]. Granzyme B cDNA was cloned into pHLseq at AgeI and KpnI sites with the forward primer 5′-GAAACCGGTGACGACGACGACAAGATCATCGGGGGACAT GAG-3′ (which introduces an enterokinase site before the amino terminus of the active protease) and the reverse primer 5′-GTGCTTGGTACCGTAGCGT TTCATGGTTTTCTT-3′. Supernatants of transfected 293T human embryonic kidney cells grown for 4 d in ExCell 293 medium (Sigma) were purified by immobilized metal affinity chromatography with nickel–nitrilotriacetic acid (Ni-NTA Superflow; Qiagen). Eluted granzyme B was treated for 16 h at 20 °C with enterokinase (0.05 IU per ml cell supernatant; Sigma). Active granzyme B was purified on an S column, then was concentrated, and its quality was assessed as described[46].

**Treatment with perforin and granzyme B.** Cells were washed and equilibrated for 5 min in cell-loading buffer (10 mM HEPES, pH 7.5, 4 mM $CaCl_2$ and 0.4% (wt/vol) BSA in Hank's balanced-salt solution) before the addition of a sublytic concentration of rat or human perforin and/or native or recombinant granzyme B diluted in perforin buffer (10 mM HEPES, pH 7.5, in Hank's balanced-salt solution). The perforin concentration was determined for each experiment as the concentration that induced 5–15% uptake of propidium iodide (2 μg/ml; Sigma) measured 20 min later by flow cytometry (FACSCalibur; Becton Dickinson)[46,48].

**Uptake of fluorescent native human granzyme B and dextran.** An Alexa Fluor 488 Microscale Protein Labeling Kit (Molecular Probes) was used for labeling of native human granzyme B. Alexa Fluor 488–granzyme B (10 μg/ml) was added with sublytic native rat perforin. Cells were then washed with PBS and were fixed before analysis by microscopy. Internalization of 10-kDa cationic TR-dextran (1.25 mg/ml; Molecular Probes) was analyzed by live-cell imaging. Dextran was added for various times with a sublytic concentration of native rat perforin. Cells were then washed with cell-loading buffer before image acquisition with a spinning-disk confocal microscope (**Supplementary Methods**).

**Time-lapse videomicroscopy and live-cell imaging.** HeLa cells were grown on collagen-coated coverslips 25 mm in diameter and were transfected overnight with plasmid encoding eGFP-tagged EEA1 or monomeric red fluorescent protein–tagged EEA1 alone or in combination with plasmid encoding eGFP-tagged wild-type Rab5, eGFP-Rab5(S34N) or Rab5(Q79L)[49] with FuGENE 6 (Roche Diagnostics). Coverslips were transferred to a sample holder (20/20 Technology) inside an environmental chamber containing the objective lenses and were maintained at 37 °C in 5% $CO_2$ and 100% humidity. Samples were treated with perforin under the microscope after acquisition with a spinning-disk confocal microscope was begun (**Supplementary Methods**).

**Detection of perforin aggregation by crosslinking.** K562 cells ($2 \times 10^5$) were washed and equilibrated for 5 min in cell-loading buffer before the addition of a sublytic concentration of native human perforin diluted in perforin buffer (10 mM HEPES, pH 7.5, in Hank's balanced-salt solution). After incubation at 37 °C, cells were transferred immediately to 4 °C and 2 mM disuccinimidyl suberate (freshly prepared; Pierce) was added. For cell fractionation, K562 cells ($4 \times 10^5$) were washed and treated with native human perforin as described above. At the appropriate time, cells were transferred to 4 °C and were centrifuged for 5 min at 300*g*. Cell pellets were incubated for 5 min in ice-cold Cell Fractionation Buffer (Ambion) before centrifugation for 5 min at 500*g* for removal of plasma membranes and nuclei. The remaining cytoplasmic fraction (supernatant) was centrifuged for 10 min at 15,000*g* to pellet cytosolic vesicles. Vesicles were resuspended in PBS before the addition of 2 mM disuccinimidyl suberate (freshly prepared). After samples were incubated for 30 min at 4 °C, 5× SDS-PAGE loading buffer was added (200 mM Tris-HCl, pH 6.8, 5% (wt/vol) SDS, 30% (vol/vol) glycerol, 0.05% (wt/vol) bromophenol blue and 10 mM β-mercaptoethanol) and samples were boiled for 5 min. Samples were separated by electrophoresis through a 4–20% denaturing gradient gel and perforin was detected by immunoblot analysis with mouse antibody to human perforin (2d4; a gift from G.M. Griffiths).

**Imaging of NK cell target cell conjugates.** YT-Indy NK cells were added to 721.221 target cells (at an effector/target ratio of 2:1) in RPMI-1640 medium containing 10% (vol/vol) FCS in 96-well V-bottomed plates, which were spun briefly and incubated for 20 min at 37 °C to allow conjugate formation (time = 0). Conjugates were then spun on poly-L-lysine-coated coverslips and were fixed with 4% (wt/vol) paraformaldehyde in PBS, then were stained as described above with monoclonal antibody to perforin (Pf-80; Mabtech) or granzyme B (GB11; Invitrogen), followed by analysis by spinning-disk confocal microscopy. For live-cell imaging, YT-Indy cells expressing eGFP-granzyme B (clone F6) were added to 721.221 target cells, followed by adherence to poly-L-lysine-coated coverslips before being imaged by widefield microscopy.

**Quantification of dextran release from endosomes and gigantosomes by fluorescent live-cell confocal microscopy.** HeLa cells seeded on collagen-coated glass coverslips 25 mm in diameter were transfected overnight with plasmid encoding eGFP-tagged EEA1. The next day, TR-dextran was added as described above with or without a sublytic concentration of native rat perforin. Coverslips were placed in an environmental chamber and were imaged by spinning-disk confocal microscopy as described above. Three-dimensional movies were obtained from a cross-section of the cells that corresponded to a *z*-stack series of five consecutive optical planes spaced by 0.7 μm acquired at a frequency of 0.05 Hz per stack series with 100 ms (eGFP) or 200 ms (dextran) of exposure time. Two-dimensional movies were then obtained by the generation of a maximum-intensity z-projection for each time point. Gigantosomes containing fluorescent dextran were identified, tracked and analyzed with Slidebook software (Intelligent Imaging) and a MATLAB routine developed in the laboratory (S.B. *et al.*, data not shown). Three sequential steps (two-dimensional Gaussian and Laplacian filtering followed by a local maximum-finding algorithm) were used for the detection of dextran-containing endosomes. Masks corresponding to the local cytosolic area surrounding the selected dextran-containing endosomes and gigantosomes were created by expansion of the endosome mask by 10 pixels in diameter and subtraction of the original endosome mask. The resulting mask had a donut shape. An identical mask was created far from any dextran-staining objects for capture of far background intensity. The intensity of the local peri-endosome and far background regions was arbitrarily set as 0 at the beginning of the time lapse movie. The intensity profile as a function of time was plotted.


46. Thiery, J., Walch, M., Jensen, D.K., Martinvalet, D. & Lieberman, J. in *Current Protocols in Cell Biology* Vol. 47 (eds. Bonifacino, J.S., Dasso, M., Harford, J.B., Lippincott-Schwartz, J. & Yamada, K.M.) Unit 3.37, 1–29 (John Wiley & Sons, Hoboken, New Jersey, 2010).
47. Aricescu, A.R., Lu, W. & Jones, E.Y. A time- and cost-efficient system for high-level protein production in mammalian cells. *Acta Crystallogr. D Biol. Crystallogr.* **62**, 1243–1250 (2006).
48. Martinvalet, D., Thiery, J. & Chowdhury, D. Granzymes and cell death. *Methods Enzymol.* **442**, 213–230 (2008).
49. Barbieri, M.A., Li, G., Mayorga, L.S. & Stahl, P.D. Characterization of Rab5:Q79L-stimulated endosome fusion. *Arch. Biochem. Biophys.* **326**, 64–72 (1996).